Original Article

DOI: 10.4274/haseki.galenos.2024.10100
Med Bull Haseki 2024;62:255-264

Predictive Value of Initial ^{18}F-FDG PET/CT for Identifying EGFR and KRAS Mutations in Patients with Non-small-cell Lung Cancer

Ozge Vural Topuz*, Nur Buyukpinarbasili**

*University of Health Sciences Turkey, Basaksehir Cam and Sakura City Hospital, Clinic of Nuclear Medicine, Istanbul, Turkey
**University of Health Sciences Turkey, Basaksehir Cam and Sakura City Hospital, Clinic of Pathology, Istanbul, Turkey

Abstract

Aim: Since the importance of epidermal growth factor receptor (EGFR) and Kirsten rat sarcoma viral oncogene homolog gene (KRAS) mutation status in predicting treatment response in non-small cell lung cancer (NSCLC) patients is well known, we aimed to evaluate whether initial fluorine-18-fluorodeoxyglucose (^{18}F-FDG) positron emission tomography-computed tomography (PET/CT) imaging could non-invasively predict EGFR or KRAS mutation states in this patient group.

Methods: This retrospective observational study examined patients with NSCLC who underwent ^{18}F-FDG PET/CT for staging from August 2021 to January 2024. Age, sex, smoking status, pathological data, EGFR and KRAS mutation status, and metabolic and volumetric PET parameters were recorded. Groups were based on gene mutation status as follows: EGFR-mutations (mt) vs. EGFR wild-type (EGFR-wt) and KRAS-mt vs. KRAS-wt.

Results: Ninety-nine patients with a mean age of 62.96±9.66 (range: 37-87) were included. The EGFR-mt group had lower metabolic tumor volume (MTV) (p=0.015) and total lesion glycolysis (TLG) (p=0.017) values. MTV had an area under the receiver operating characteristic curve (AUC) of 0.667 [95% confidence interval (CI): 0.547-0.788, p=0.015], and with a ≤24.9 cut-off, yielded 60.87% sensitivity, 68.42% specificity, and 66.67% accuracy to detect EGFR-mt. For TLG, the AUC was 0.664 (95% CI: 0.540-0.788, p=0.017) and a ≤408.1 cut-off yielded 86.96% sensitivity, 43.42% specificity, 53.54% accuracy, and 91.67% NPV. KRAS-mt was detected in 34 (34.34%) patients, and there were no significant differences between the KRAS-mt and KRAS-wt groups in terms of PET parameters.

Conclusion: Primary tumor parameters derived from initial ^{18}F-FDG PET/CT can predict EGFR mutation status but not KRAS mutation status. The high negative predictive value of TLG can be used to rule out EGFR-mt status, possibly preventing unnecessary treatments in patients without favorable genetic properties, especially when genetic analyses are not possible.

Keywords: Lung cancer, non-small-cell lung cancer, ^{18}F-FDG PET/CT, EGFR, KRAS

Introduction

Lung cancer is one of the leading causes of cancer-related deaths worldwide, with approximately 85% of patients suffering from non-small-cell lung cancer (NSCLC) (1). Tyrosine kinase inhibitors (TKIs) have been shown to improve NSCLC outcomes (2), and it has been established that a kinase domain mutation of the epidermal growth factor receptor (EGFR) is associated with a favorable response to TKIs. In fact, progression-free survival (PFS) is longer with the use of TKIs compared with chemotherapy in patients with EGFR mutations (EGFR-mt) (3). The Kirsten rat sarcoma viral oncogene homolog gene (KRAS) encodes a member of the small GTPase superfamily that has an impact on the EGFR pathway. Mutations in this gene (KRAS-mt) are associated with an unfavorable response to TKIs (4).

Fluorine-18-fluorodeoxyglucose (^{18}F-FDG) positron emission tomography-computed tomography (PET/CT)

Address for Correspondence: Ozge Vural Topuz, University of Health Sciences Turkey, Basaksehir Cam and Sakura City Hospital, Clinic of Nuclear Medicine, Istanbul, Turkey
E-mail: ozgevuraltopuz@gmail.com **ORCID:** orcid.org/0000-0001-7197-5866
Received: 30.09.2024 **Accepted:** 12.12.2024

a non-invasive molecular imaging method that is widely used for staging, response assessment, and recurrence detection in NSCLC (5). The EGFR mutation status plays an important role in the management of patients with advanced NSCLC; regardless of other factors, the molecular profiling of EGFR is essential to guide clinical treatment (6). However, obtaining high-quality tumor tissue for EGFR-mt testing is difficult in many cases, given the shortage of biopsy samples and the physical condition of patients. Therefore, a non-invasive and simple method to identify EGFR-mt is necessary to inform treatment decisions. Recent studies, the results of which are still controversial, have focused on whether EGFR-mt and KRAS-mt states can be associated with metabolic parameters obtained via ^{18}F-FDG PET/CT, especially the maximum standardized uptake value (SUV_{max}) (5,7). Few reports have explored the utility of metabolic tumor volume (MTV) and total lesion glycolysis (TLG) values in this context, and these studies have revealed inconsistent findings (8).

We hypothesized that initial ^{18}F-FDG PET/CT parameters obtained from the primary lesion could be utilized to predict the presence or absence of EGFR-mt or KRAS-mt in patients with NSCLC.

Methods

Study Design and Patients

This study was approved by the Clinical Research Ethics Committee of University of Health Sciences Turkey, Basaksehir Cam and Sakura City Hospital (date: July 2023, approval no.: 2023.07.296). Informed consent was obtained from all participants included in the study. Diagnostic and therapeutic procedures were performed in accordance with national guidelines and the principles of the Declaration of Helsinki (1964). All patients received appropriate information and provided written informed consent.

This retrospective observational cohort study examined patients with NSCLC who underwent ^{18}F-FDG PET/CT imaging for staging purposes at baseline between August 2021 and January 2024. The inclusion criteria were as follows: pathologically confirmed diagnosis of NSCLC, being treatment-naïve before ^{18}F-FDG PET/CT imaging, confirmation of EGFR-mt and KRAS-mt status within 1 month from the time of imaging, and availability of all relevant clinical and imaging data. The exclusion criteria were having received any antitumor therapy before ^{18}F-FDG PET/CT, having a history of other malignancies, having comorbidities affecting the metabolic parameters examined by ^{18}F-FDG PET/CT (such as diabetes mellitus), and having pneumonia or other infections that might confound the analyses (Figure 1).

Age, sex, smoking characteristics (pack years), histopathology, clinical stage, primary tumor site, nodal involvement, metastasis, operation history, molecular analysis results concerning EGFR and KRAS (mutations), and metabolic and volumetric parameters derived from ^{18}F-FDG PET/CT were recorded. The cancer stage was determined according to the 8th TNM classification for lung and pleural tumors (9).

Patients were classified according to mutation status as EGFR-mt and EGFR wild type (EGFR-wt) or KRAS-mt and KRAS wild type (EGFR-wt). The specimens were defined as EGFR-mt if mutations were identified in exons 18, 19, 20, and 21. The presence of KRAS-mt was determined by detecting mutations in KRAS codons 12, 13, and 61.

^{18}F-FDG PET/CT Procedure

Imaging was performed after at least 6 h of fasting and the presence of a glucose level of <150 mg/dL. After ^{18}F-FDG injection, patients were left to rest for 50 min before imaging with the Ingenuity TF 64 scanner (Philips Medical Systems, OH, USA). Low-dose CT was performed with the following settings: 113 mAs, 120 kV, and 4-mm section thickness. The PET images were recorded in the caudocranial axis on the identical transverse field of view for a duration of 3 min per bed, and corrections for attenuation were based on the initial CT images. All obtained images (PET, CT, corrected, and uncorrected) were assessed on maximum intensity projection images as well as transaxial, coronal, and sagittal cross-sectional images. Reconstructions were performed according to the EANM procedure guidelines for tumor imaging (version 2.015) (10).

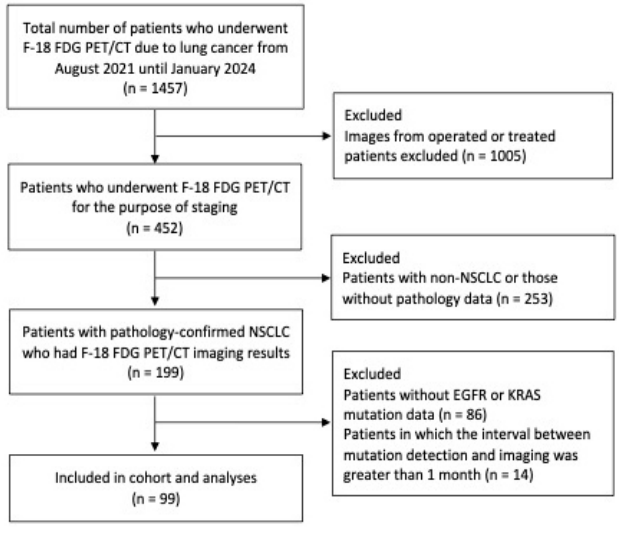

Figure 1. Flowchart of the study

Imaging Assessment

For the evaluation of images, a volume of interest (VOI) including all relevant tissue was delineated on attenuation-corrected ^{18}F-FDG PET/CT images of the primary tumor (automated contouring and manual correction) in the axial, sagittal, and coronal planes (Figure 2).

SUV_{max} was defined as the highest SUV measured from any voxel within the VOI. The mean SUV (SUV_{mean}) was defined as the SUV inside the VOI. The MTV was recorded with a threshold of 40% (of the SUV_{max}) within the VOI, and TLG was calculated by multiplying the MTV by the SUV_{mean}. To normalize FDG uptake, three spherical regions of interest (ROIs) with a diameter of 3 cm were placed in sites with homogenous FDG uptake inside the right lobe of the liver, and the mean value was calculated (liver-SUV_{mean}). The lung-to-liver ratio (SUV_{max}/liver-SUV_{mean}) was then calculated to generate normalized SUV data. All evaluations and calculations were performed by two nuclear medicine physicians who were blinded to the study data.

Pathologic Evaluation

Genomic DNA was extracted from formalin-fixed, paraffin-embedded non-small-cell lung carcinoma tissues, and EGFR-mt were detected using real-time PCR. Tissues were sectioned to 5 µm, deparaffinized, and then subjected to genomic DNA analysis using a DNA sample preparation kit according to the manufacturer's instructions. Following quantification of genomic DNA, real-time PCR was carried out to amplify the target area and detect the targeted mutations in exon 18 (G719A, G719C, and G719S), 19 (deletions and complex mutations), 20 (S768I, T790M, and insertions), and 21 (L858R and L861Q) using the EGFR mutation test (v2) on the Cobas® z480 analyzer, which were automatically analyzed and output by Cobas® 4800 software. For KRAS, we also used real-time PCR to detect targeted mutations. Additionally, we detected mutations in codons 12 and 13 of exon 2 and 61 of exon 3 in the KRAS gene using the KRAS mutation test on Cobas® z480 analyzer, which were again automatically analyzed and collected using the same software.

Statistical Analysis

All analyses were performed on IBM SPSS Statistics for Windows, Version 25.0 (IBM Corp., Armonk, NY, USA). For the normality check, the Kolmogorov-Smirnov test was used. Descriptive statistics were presented by using mean ± standard deviation for normally distributed continuous variables, median (25^{th} percentile-75^{th} percentile) for non-normally distributed continuous variables, and frequency (percentage) for categorical variables. Normally distributed variables were analyzed with the Student's t-test. Non-normally distributed variables were analyzed using the Mann-Whitney U test. Categorical variables were analyzed using the chi-square tests, the Fisher-Freeman-Halton test, or Fisher's exact test. Prediction performances were assessed using receiver operating characteristic (ROC) curve analysis. The optimal cut-off points were determined using the Youden index. Logistic regression analyses were performed to identify factors independently associated with EGFR and KRAS mutations. Variables were initially analyzed by univariate regression analysis, and those showing significance were included in the multivariate model. Detection of $p<0.05$ values was accepted to show statistically significant.

Results

We included 99 patients (77 males and 22 females) in our study; the mean age was 62.96±9.66 (range 37-87) years. Seventy-six (84.44%) patients had a smoking history. Most cases (71.72%) involved adenocarcinoma. Fifty-one (51.52%) patients were stage T4, 45 (45.45%) were stage N3, 54 (54.55%) had metastasis, and 54 (54.55%) were clinical stage IV. The right lung (63.64%) and upper lobe (53.54%) were the most common sites of primary lesions. The bone was the most common site of metastasis (31.31%). Ten (10.10%) patients underwent surgical treatment. EGFR and KRAS mutations (EGFR-mt and KRAS-mt) were detected in 23 (23.23%) and 34 (34.34%) patients, respectively (Table 1).

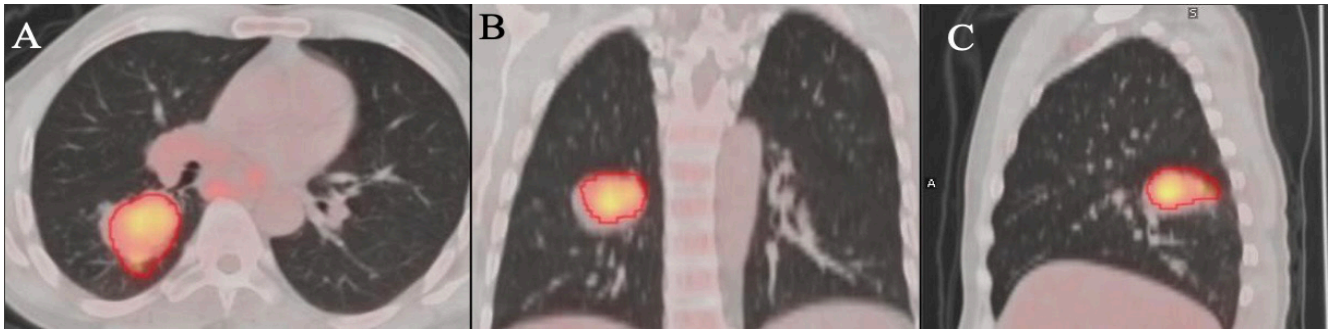

Figure 2. A VOI of the primary tumor in the axial (a), coronal (b), and sagittal (c) planes
VOI: Volume of interest

Table 1. Summary of variables	
Age	62.96±9.66
Sex	
Male	77 (77.78%)
Female	22 (22.22%)
Smoking	76 (84.44%)
Pack year	30 (20-48)
Histopathology	
Adenocarcinoma	71 (71.72%)
SCC	28 (28.28%)
T stage	
T1	5 (5.05%)
T2	25 (25.25%)
T3	18 (18.18%)
T4	51 (51.52%)
N stage	
N0	14 (14.14%)
N1	15 (15.15%)
N2	25 (25.25%)
N3	45 (45.45%)
M stage	
M0	45 (45.45%)
M1	54 (54.55%)
Clinical stage	
Stage I	4 (4.04%)
Stage II	5 (5.05%)
Stage III	36 (36.36%)
Stage IV	54 (54.55%)
Side	
Right	63 (63.64%)
Left	36 (36.36%)
Lobe	
Upper	53 (53.54%)
Middle	6 (6.06%)
Lower	40 (40.40%)
Metastasis location*	54 (54.55%)
Distant lymph node	16 (16.16%)
Contralateral lung	4 (4.04%)
Brain	19 (19.19%)
Liver	9 (9.09%)
Bone	31 (31.31%)
Adrenal gland	13 (13.13%)
Other	3 (3.03%)
Operation	10 (10.10%)
EGFR mutation	23 (23.23%)
Exon 18 G719X:	2 (2.02%)
Exon 19 deletion	17 (17.17%)
Exon 20 insertion	1 (1.01%)
Exon 21 L858R:	3 (3.03%)
KRAS mutation	34 (34.34%)
Codon 12	19 (19.19%)
Codon 13	1 (1.01%)
Codons 12 and 13	9 (9.09%)
Codon 61	5 (5.05%)
SUV_{mean}	6.4 (4.8-9.9)
SUV_{max}	11.4 (8.3-16.9)
MTV	36.0 (14.6-74.3)
TLG	281.88 (81.00-592.9)
Liver-SUV_{mean}	2.00±0.43
Normalized SUV	5.93 (4.29-8.10)

Descriptive statistics were presented by using mean ± standard deviation for normally distributed continuous variables, median (25^{th}-75^{th} percentiles) for non-normally distributed continuous variables, and frequency (percentage) for categorical variables. *Patients may have more than one of the following
SCC: Squamous cell carcinoma, MTV: Metabolic tumor volume, TLG: Total lesion glycolysis

Association between EGFR status, clinical features, and PET/CT results

Female frequency (p<0.001) was significantly higher in the EGFR-mt group than in the EGFR-wt group. Smoking frequency (p<0.001) and pack years (p=0.003) were significantly lower in the EGFR-mt group than in the EGFR-wt group. We found no significant differences between the EGFR mutation groups in terms of age, histopathology, T stage, N stage, M stage, clinical stage, side, lobe, and surgery percentages (Table 2).

MTV (p=0.015) and TLG (p=0.017) were significantly lower in the EGFR-mt group than in the EGFR-wt group. We found no significant differences between the EGFR mutation groups in terms of SUV_{mean}, SUV_{max}, liver-SUV_{mean}, and normalized SUV (Table 2).

When we evaluated the EGFR-mt prediction performance of the PET parameters, MTV had 60.87% sensitivity, 68.42% specificity, 66.67% accuracy, 36.84% positive predictive value (PPV), and 85.25% negative predictive value (NPV) for a cut-off value of 24.9 (equal or lower values represent the presence of EGFR mutation).

Table 2. Summary of variables associated with EGFR mutation			
	EGFR mutation		
	Negative (n=76)	**Positive (n=23)**	**p-value**
Age	62.83±9.33	63.39±10.91	0.808†
Sex			
Male	69 (90.79%)	8 (34.78%)	<0.001§
Female	7 (9.21%)	15 (65.22%)	
Smoking	65 (92.86%)	11 (55.00%)	<0.001§
Pack year	35 (20-50)	17.5 (0-30)	0.003‡
Histopathology			
Adenocarcinoma	52 (68.42%)	19 (82.61%)	0.289§
SCC	24 (31.58%)	4 (17.39%)	
T stage			
T1	2 (2.63%)	3 (13.04%)	0.080#
T2	17 (22.37%)	8 (34.78%)	
T3	16 (21.05%)	2 (8.70%)	
T4	41 (53.95%)	10 (43.48%)	
N stage			
N0	11 (14.47%)	3 (13.04%)	0.868#
N1	11 (14.47%)	4 (17.39%)	
N2	18 (23.68%)	7 (30.43%)	
N3	36 (47.37%)	9 (39.13%)	
M stage			
M0	36 (47.37%)	9 (39.13%)	0.648§
M1	40 (52.63%)	14 (60.87%)	
Clinical stage			
Stage I	2 (2.63%)	2 (8.70%)	0.305#
Stage II	5 (6.58%)	0 (0.00%)	
Stage III	29 (38.16%)	7 (30.43%)	
Stage IV	40 (52.63%)	14 (60.87%)	
Side			
Right	48 (63.16%)	15 (65.22%)	1.000§
Left	28 (36.84%)	8 (34.78%)	
Lobe			
Upper	41 (53.95%)	12 (52.17%)	0.928#
Middle	5 (6.58%)	1 (4.35%)	
Lower	30 (39.47%)	10 (43.48%)	
Operation	7 (9.21%)	3 (13.04%)	0.694¶
SUV_{mean}	6.7 (4.9-10.0)	5.8 (4.4-8.6)	0.272‡
SUV_{max}	11.75 (8.35-17.15)	9.8 (7.3-14.3)	0.208‡
MTV	42.6 (19.1-83.1)	18.1 (8.7-43.6)	0.015‡
TLG	355.77 (86.82-677)	138.06 (33.11-384.56)	0.017‡
Liver-SUV_{mean}	1.97±0.43	2.09±0.44	0.239†
Normalized SUV	6.32 (4.51-8.32)	4.62 (4.19-6.93)	0.063‡

Descriptive statistics were presented by using mean ± standard deviation for normally distributed continuous variables, median (25^{th}-75^{th} percentile) for non-normally distributed continuous variables, and frequency (percentage) for categorical variables.
†Student's t-test, ‡Mann-Whitney U test, chi-square test, #Fisher-Freeman-Halton test, Fisher's exact test

The area under the ROC curve (AUC) was 0.667 [95% confidence interval (CI): 0.547-0.788, p=0.015]. TLG had 86.96% sensitivity, 43.42% specificity, 53.54% accuracy, 31.75% PPV, and 91.67% NPV for a cut-off value of 408.1 (equal or lower values represent the presence of EGFR mutation). The AUC was 0.664 (95% CI: 0.540-0.788, p=0.017) (Figure 3).

The SUV_{mean}, SUV_{max}, and normalized SUV were non-significant in distinguishing patients with or without EGFR-mt (Table 3).

According to the multivariable logistic regression analysis, female sex was the only factor independently associated with EGFR-mt (OR: 12.882, 95% CI: 2.922-56.796, p=0.001) (Table 4).

The baseline PET/CT images of a patient with EGFR-mt infection are presented in Figure 4, and those of a patient with EGFR-wt infection are presented in Figure 5.

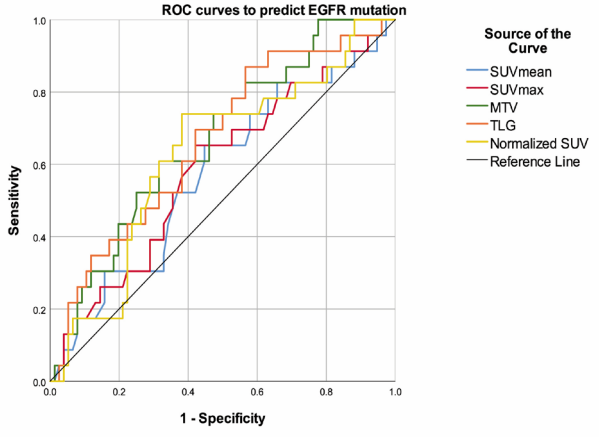

Figure 3. ROC curves of PET findings for EGFR mutation prediction

ROC: Receiver operating characteristic, PET: Positron emission tomography, EGFR: Epidermal growth factor receptor

Table 3. Performance of PET in predicting EGFR mutation, ROC curve analysis

	Cut-off	Sensitivity	Specificity	Accuracy	PPV	NPV	AUC (95% CI)	p-value
SUV_{mean}	**≤6.3**	**65.22%**	**55.26%**	**57.58%**	**30.61%**	**84.00%**	**0.576 (0.441-0.710)**	**0.272**
SUV_{max}	≤10.9	65.22%	57.89%	59.60%	31.91%	84.62%	0.587 (0.453-0.720)	0.208
MTV	≤24.9	60.87%	68.42%	66.67%	36.84%	85.25%	0.667 (0.547-0.788)	0.015
TLG	≤408.1	86.96%	43.42%	53.54%	31.75%	91.67%	0.664 (0.540-0.788)	0.017
Normalized SUV	≤5.59	73.91%	61.84%	64.65%	36.96%	88.68%	0.628 (0.499-0.758)	0.063

PPV: Positive predictive value, NPV: Negative predictive value, AUC: Area under the curve, ROC: Receiver operating characteristic, CI: Confidence interval, PET: Positron emission tomography, EGFR: Epidermal growth factor receptor

Table 4. Odds ratios for the EGFR mutation and logistic regression analysis

	Univariable		Multivariable	
	OR (95% CI)	**p-value**	**OR (95% CI)**	**p-value**
Age	1.006 (0.958-1.056)	0.806		
Sex, Female	18.482 (5.806-58.833)	<0.001	12.882 (2.92256.796)	0.001
Smoking	0.094 (0.027-0.334)	<0.001	0.427 (0.078-2.339)	0.327
Histopathology, adenocarcinoma	2.192 (0.672-7.147)	0.193		
T stage	0.641 (0.401-1.025)	0.063		
N stage	0.933 (0.609-1.427)	0.748		
M stage	1.400 (0.541-3.623)	0.488		
Clinical stage	1.048 (0.565-1.943)	0.883		
Side, left	0.914 (0.344-2.428)	0.857		
Lobe, lower	1.179 (0.459-3.032)	0.732		
Operation	1.479 (0.350-6.248)	0.595		
SUV_{mean}, ≤6.3	2.316 (0.878-6.109)	0.090		
SUV_{max}, ≤10.9	2.578 (0.976-6.811)	0.056		
MTV, ≤24.9	3.370 (1.281-8.865)	0.014	1.503 (0.336-6.717)	0.594
TLG, ≤408.1	5.116 (1.401-18.689)	0.014	1.157 (0.182-7.381)	0.877
Normalized SUV, ≤5.59	4.592 (1.624-12.984)	0.004	1.320 (0.284-6.143)	0.724

OR: Odds ratio, CI: Confidence interval, EGFR: Epidermal growth factor receptor

Association between KRAS status, clinical features, and PET/CT results

Adenocarcinoma (p=0.001) percentage was significantly higher in the KRAS-mt group than in the KRAS-wt group. We found no significant differences between the KRAS mutation groups in terms of age, sex, smoking status, pack years, T stage, N stage, M stage, clinical stage, side, lobe, or surgical treatment. In addition, there were no significant differences between the KRAS mutation groups in terms of SUV_{mean}, SUV_{max}, MTV, TLV, liver-SUV_{mean}, and normalized SUV (Table 5).

Logistic regression analysis revealed that adenocarcinoma was the only factor associated with the presence of KRAS-mt (OR: 10.667, 95% CI: 2.351-48.396, p=0.002).

Discussion

In light of the advances and diversity in the treatment of NSCLC, such as TKIs, it is crucial to identify favorable mutations in the early stages of the disease. Although genetic analysis is undoubtedly the best approach, the use of molecular profiling may be limited due to various factors, including difficulty in obtaining sufficient tumor tissue, unavailability of genetic analyses, and the invasiveness of the procedure (4,6). The current study reported that it may be possible to obtain information regarding the presence/absence of relevant mutations by evaluating metabolic parameters obtained from ^{18}F-FDG PET/CT imaging performed at baseline. MTV and TLG were found to have statistical significance in distinguishing patients with and without EGFR-mt, but not KRAS-mt. Although the overall accuracy values were not excellent for distinguishing the presence of EGFR mutations, TLG had exceptional sensitivity and NPV, indicating notable utility in detecting and ruling out the presence of favorable EGFR mutations among patients with NSCLC.

In our study, similar to the literature, female sex, low smoking percentage, as well as PET parameters such as MTV and TLG obtained from the primary lesion, were significantly lower in patients with EGFR-mt compared with those without (7,11,12). Additionally, the MTV and TLG values obtained from the initial imaging of the primary lesions were significantly lower in the EGFR-mt group.

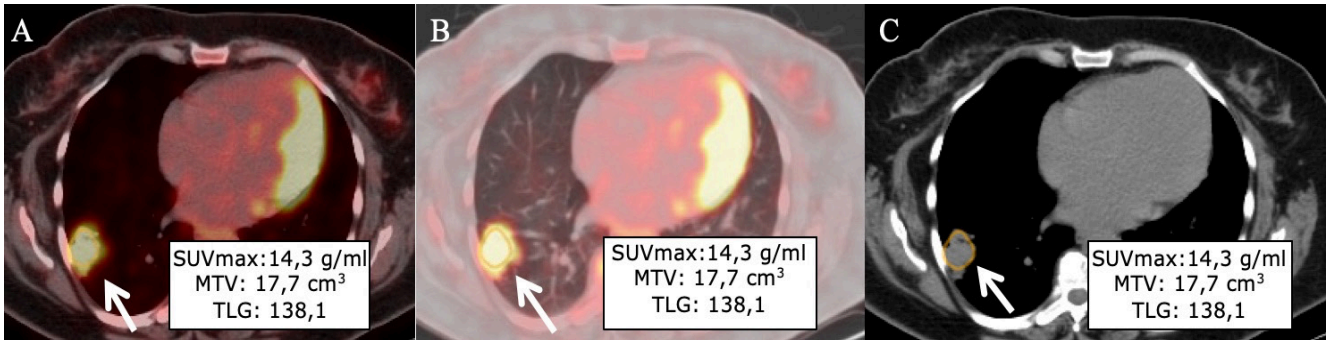

Figure 4. Pretreatment ^{18}F-FDG PET/CT images of a patient with NSCLC and EGFR mutation, demonstration of SUVmax, MTV, and TLG values derived from the primary lung tumor (arrow) on axial fused images (a,b) and axial CT images (c)

^{18}F-FDG PET/CT: Fluorine-18-fluorodeoxyglucose positron emission tomography-computed tomography, NSCLC: Non-small-cell lung cancer, EGFR: Epidermal growth factor receptor, MTV: Metabolic tumor volume, TLG: Total lesion glycolysis, CT: Computed tomography

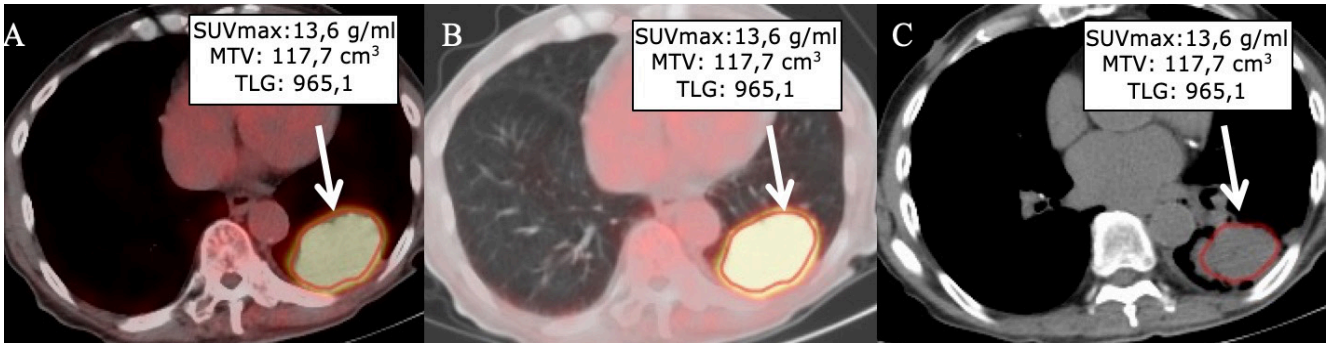

Figure 5. Pretreatment ^{18}F-FDG PET/CT images of a patient with NSCLC without EGFR mutation, demonstration of the SUVmax, MTV, and TLG values derived from the primary lung tumor (arrow) on the axial fused images (a,b) and axial CT images (c)

^{18}F-FDG PET/CT: Fluorine-18-fluorodeoxyglucose positron emission tomography-computed tomography, NSCLC: Non-small-cell lung cancer, EGFR: Epidermal growth factor receptor, MTV: Metabolic tumor volume, TLG: Total lesion glycolysis, CT: Computed tomography

Table 5. Summary of variables associated with KRAS mutation			
	KRAS mutation		
	Negative (n=65)	**Positive (n=34)**	**p-value**
Age	62.92±9.59	63.03±9.95	0.959†
Sex			
Male	47 (72.31%)	30 (88.24%)	0.120§
Female	18 (27.69%)	4 (11.76%)	
Smoking	47 (79.66%)	29 (93.55%)	0.126¶
Pack year	30 (15-45)	35 (20-50)	0.341‡
Histopathology			
Adenocarcinoma	39 (60.00%)	32 (94.12%)	0.001§
SCC	26 (40.00%)	2 (5.88%)	
T stage			
T1	3 (4.62%)	2 (5.88%)	1.000#
T2	17 (26.15%)	8 (23.53%)	
T3	12 (18.46%)	6 (17.65%)	
T4	33 (50.77%)	18 (52.94%)	
N stage			
N0	9 (13.85%)	5 (14.71%)	0.685§
N1	11 (16.92%)	4 (11.76%)	
N2	18 (27.69%)	7 (20.59%)	
N3	27 (41.54%)	18 (52.94%)	
M stage			
M0	27 (41.54%)	18 (52.94%)	0.385§
M1	38 (58.46%)	16 (47.06%)	
Clinical stage			
Stage I	2 (3.08%)	2 (5.88%)	0.664#
Stage II	3 (4.62%)	2 (5.88%)	
Stage III	22 (33.85%)	14 (41.18%)	
Stage IV	38 (58.46%)	16 (47.06%)	
Side			
Right	38 (58.46%)	25 (73.53%)	0.208§
Left	27 (41.54%)	9 (26.47%)	
Lobe			
Upper	34 (52.31%)	19 (55.88%)	0.221#
Middle	6 (9.23%)	0 (0.00%)	
Lower	25 (38.46%)	15 (44.12%)	
Operation	5 (7.69%)	5 (14.71%)	0.305¶
SUV_{mean}	6.3 (4.7-10.6)	6.5 (5.2-9.3)	0.897‡
SUV_{max}	11.0 (8.1-17.7)	11.45 (8.4-16.9)	0.909‡
MTV	33.0 (17.7-71.9)	41.4 (12.4-83.0)	0.912‡
TLG	281.88 (84.68-534.60)	261.60 (74.80-642.60)	0.848‡
Liver-SUV_{mean}	2.00±0.39	1.99±0.51	0.834†
Normalized SUV	5.59 (4.19-9.13)	6.32 (4.62-7.52)	0.757‡

Descriptive statistics were presented by using mean ± standard deviation for normally distributed continuous variables, median (25^{th}-75^{th} percentiles) for non-normally distributed continuous variables, and frequency (percentage) for categorical variables.
†Student's t-test, ‡Mann-Whitney U test, : chi-square test, #Fisher-Freeman-Halton test, : Fisher's exact test, KRAS: Kirsten rat sarcoma viral oncogene homolog gene, SCC: Squamous cell carcinoma, MTV: Metabolic tumor volume, TLG: Total lesion glycolysis

This relationship is likely due to the effect of EGFR on glucose transporters in the cell membrane via downstream pathways that may affect tumor glucose metabolism. In previous studies, different results were presented when examining the role of SUV_{max} in predicting EGFR mutation in patients with NSCLC.

Most studies have reported higher frequencies of EGFR mutations in patients with lower SUV values (12,13). However, a study consisting of Asian patients with advanced lung adenocarcinoma reported that patients with higher SUV_{max} values were more likely to carry EGFR-mt (14). Wang et al. (15) also reported significantly higher SUV_{max} values in patients with NSCLC with EGFR mutations compared with those without mutations, which they attributed to increased glucose uptake. These varying results suggest that SUV_{max} values in the present study may be affected by a multitude of factors, such as patient characteristics and imaging technique. As such, we believe that incorporating parameters like MTV and TLG could be beneficial for the evaluation and management of this patient group. Additionally, ethnic differences in patient groups and other uncontrolled genetic mutations in the EGFR-wt group may also cause these differences. Liu et al. (16), supporting this perspective and similar to our study, found that MTV values were lower in the EGFR-mt. However, the authors did not find a correlation between SUV_{max} and mutation status, thereby providing credibility to the perceived impact of similar underlying reasons. The authors suggested that this may be due to the semiquantitative nature of SUV data, which might vary depending on the PET scanner, fasting time, plasma glucose level, and selected ROIs (16).

In contrast to our findings, Minamimoto et al. (8) found that SUV_{max} values of primary lesions were predictive of EGFR-mt, whereas MTV and TLG were not, suggesting that gene mutations were unassociated with tumor size or volume. However, most of the patients included in their study (70.2%) had clinical stages of IA or IB, whereas 91% of the patients in our study had stage III and IV. The difference in the severity of patients is an important factor that could explain the contrasting results (8).

Our study demonstrated no correlation between ^{18}F-FDG uptake and KRAS-mt status, which is consistent with several other studies previously reported in the literature (8,17). Interestingly, Caicedo et al. (18), in their study enrolling patients with stage III and IV NSCLC, reported that SUV values were significantly higher in the KRAS-mt group than in the KRAS-wt group. Further studies with larger cohorts are required to clarify the associations between PET parameters and KRAS-mt states.

Since there are many variables affecting SUV_{max} values, such as body size and amount of tracer injected, standardization of SUV_{max} by assessing liver SUV data, as well as other approaches, is known to reduce variability. It has been reported to improve prognosis prediction and treatment response assessment in NSCLC (19). Mak et al. (20) reported that normalized SUV_{max} values of the primary tumor (normalized for SUV of blood in the pulmonary artery) were predictive of EGFR mutation. In our study, similar to the SUV values, there was no significant difference between the mutation groups when we used normalized SUV values. Since the utility of this approach has not been validated in this particular patient group, more studies are needed to determine whether normalized SUV values differ from other metabolic parameters in predicting genetic mutations in NSCLC.

In our study, based on the exceptionally high NPV of TLG in predicting EGFR-mt (91.6% for a cut-off point of 408.1), it may be feasible to suggest that early ^{18}F-FDG PET/CT imaging data can be used to primarily predict the absence of EGFR mutations, thereby facilitating the noninvasive identification of patients that will not respond to TKI in the early stages of the disease. With this approach, treatment options suitable for the appropriate patient group can be determined, and unnecessary treatments can be prevented when genetic analyses are unavailable or cannot be performed. Prospective studies with a larger number of patients are needed to confirm this finding.

Study Limitations

One of the limitations of our study was its retrospective design, which included a relatively small number of patients. Second, we could not report the prognostic value of ^{18}F-FDG PET/CT because the prognosis of the patients was not yet determined. Despite these limitations, our study has identified a non-invasive ^{18}F-FDG PET/CT parameter that can predict patients with NSCLC who are unlikely to respond to treatment.

Conclusion

Our study revealed that it is possible to noninvasively predict the presence/absence of EGFR mutations in the early period of the disease using the MTV and TLG values extracted from baseline ^{18}F-FDG PET/CT imaging. Since the sensitivity and NPV of TLG were exceptionally high, it may be possible to rule out the presence of EGFR mutations using this approach. It is evident that these results are relevant in cases in which genetic detection is not feasible and could prevent unnecessary treatments by identifying patients without EGFR-mt who do not demonstrate favorable response to TKIs.

Ethics

Ethics Committee Approval: This study was approved by the Ethics Committee of University of Health Sciences Turkey, Basaksehir Cam and Sakura City Hospital (date: July 2023, approval no.: 2023.07.296).

Informed Consent: Informed consent was obtained from all participants included in the study.

Footnotes

Authorship Contributions

Surgical and Medical Practices: O.V.T., N.B., Concept: O.V.T., Design: O.V.T., Data Collection or Processing: O.V.T., N.B., Analysis or Interpretation: O.V.T., Literature Search: O.V.T., Writing: O.V.T., N.B.

Conflict of Interest: No conflicts of interest were declared by the authors.

Financial Disclosure: This study received no financial support.

References

1. Siegel RL, Miller KD, Fuchs HE, Jemal A. Cancer statistics, 2022. CA Cancer J Clin. 2022;72:7-33.
2. Ettinger DS, Wood DE, Aisner DL, et al. Non-Small Cell Lung Cancer, Version 3.2022, NCCN Clinical Practice Guidelines in Oncology. J Natl Compr Canc Netw. 2022;20:497-530.
3. Mok T, Jänne PA, Nishio M, et al. HERTHENA-Lung02: phase III study of patritumab deruxtecan in advanced *EGFR*-mutated NSCLC after a third-generation EGFR TKI. Future Oncol. 2024;20:969-80.
4. Zheng J, Dou Y, Huang D, et al. Overall signature of acquired KRAS gene changes in advanced non-small cell lung cancer patient with EGFR-TKI resistance. Jpn J Clin Oncol. 2024;54:89-96.
5. Park JS, Park HY, Choi Y. Effect of Epidermal Growth Factor Receptor Mutation on Positron Emission Tomography/ Computed Tomography in Lung Cancer. Anticancer Res. 2024;44:2681-7.
6. Zhang X, Zhang G, Qiu X, et al. Non-invasive decision support for clinical treatment of non-small-cell lung cancer using a multiscale radionics approach. Radiother Oncol. 2024;191:110082.
7. Lee SM, Bae SK, Jung SJ, Kim CK. FDG uptake in non-small cell lung cancer is not an independent predictor of EGFR or KRAS mutation status: a retrospective analysis of 206 patients. Clin Nucl Med. 2015;40:950-8.
8. Minamimoto R, Jamali M, Gevaert O, et al. prediction of EGFR and KRAS mutation in non-small-cell lung cancer using quantitative 18F FDG-PET/CT metrics. Oncotarget. 2017;8:52792-801.
9. Detterbeck FC, Boffa DJ, Kim AW, Tanoue LT. The Eighth Edition Lung Cancer Stage Classification. Chest. 2017;151:193-203.
10. Boellaard R, Delgado-Bolton R, Oyen WJ, et al. FDG PET/CT: EANM procedure guidelines for tumour imaging: version 2.0. Eur J Nucl Med Mol Imaging. 2015;42:328-54.
11. Moorthi S, Paguirigan A, Itagi P, et al. The genomic landscape of lung cancer in never-smokers from the Women's Health Initiative. JCI Insight. 2024;9:e174643.
12. Wang J, Wen X, Yang G, et al. Predictive value of 18F-FDG PET/CT in patients with EGFR-mutated lung adenocarcinoma population. Transl Cancer Res. 2022;11:2338-47.
13. Whi W, Ha S, Bae S, et al. Relationship between EGFR Mutation and Metabolic Activity and Asphericity of Metabolic Tumor Volume in Lung Adenocarcinoma. Nucl Med Mol Imaging. 2020;54:175-82.
14. Huang CT, Yen RF, Cheng MF, et al. Correlation between F-18 fluorodeoxyglucose-positron emission tomography maximal standardized uptake value and EGFR mutations in advanced lung adenocarcinoma. Med Oncol. 2010;27:9-15.
15. Wang Y, Han R, Wang Q, et al. Biological significance of 18F-FDG PET/CT maximum standard uptake value for predicting EGFR mutation status in non-small cell lung cancer patients. Int J Gen Med. 2021;14:347-56.
16. Liu A, Han A, Zhu H, et al. The role of metabolic tumor volume (MTV) measured by (18F) FDG PET/CT in predicting EGFR gene mutation status in non-small cell lung cancer. Oncotarget. 2017;8:33736-44.
17. Takamochi K, Mogushi K, Kawaji H, et al. Correlation of EGFR or KRAS mutation status with 18F-FDG uptake on PET-CT scan in lung adenocarcinoma. PLoS One. 2017;12:e0175622.
18. Caicedo C, Garcia-Velloso MJ, Lozano MD, et al. Role of (^{18}F) FDG PET in the prediction of KRAS and EGFR mutation status in patients with advanced non-small-cell lung cancer. Eur J Nucl Med Mol Imaging. 2014;41:2058-65.
19. Zhang P, Chen W, Zhao K, et al. Tumor to liver maximum standardized uptake value ratio of FDG-PET/CT parameters predicts tumor treatment response and survival of stage III non-small cell lung cancer. BMC Med Imaging. 2023;23:107.
20. Mak RH, Digumarthy SR, Muzikansky A, et al. Role of 18F-fluorodeoxyglucose positron emission tomography for predicting epidermal growth factor Receptor mutations in non-small-cell lung cancer. Oncologist. 2011;16:319-26.